

# A Temperature and Strain Rate Dependent Material Model with Tension-Compression Asymmetry for 0.25 inch Ti-6Al-4V Plate

Leyu Wang<sup>1)</sup>, Paul DuBois<sup>1)</sup>, Kelly Carney<sup>1)</sup>, Cing-Dao Kan<sup>1)</sup>  
<sup>1</sup>Center of Collision Safety and Analysis, George Mason University, USA

## Abstract

*Tension-compression asymmetry observed in a 0.25" thick Titanium plate is modeled with \*MAT\_224\_GYS, an isotropic elastic-thermo-viscous-plastic material model in LS-DYNA®. The input deck fits a series of tensile and compression tests at different strain rates and temperatures, conducted on samples cut from a 0.25" commercial off-the-shelf titanium plate. The rate and temperature dependent hardening law is separately defined for the tension and compression response. It is seen that \*MAT\_224\_GYS is capable of capturing the tension-compression asymmetry of Titanium Ti-6Al-4V.*

## 1. Introduction

The 0.25" plate of Titanium Alloy Ti-6Al-4V has tension-compression asymmetry in plasticity (r.f. Figure 1). Classical continuum mechanics(Liu, 2002)(Eringen, 1980) does not predict an asymmetric isotropic flow law for metal. Classical isotropic material models can fit either tension or compression, but not both at the same time. In impact analysis, both tension and compression should be captured accurately in order to predict the deformation and failure of different impact velocities and projectile shapes. To do that, the rate and temperature dependent hardening law needs to be defined separately in the tension and compression directions.

On the microscopic level, the origin of the anisotropy is believed to occur during the grain refinement in the rolling process, where a visible directional difference is observed (r.f. Figure 2). Difference in rolling process will produce differences in microstructure and therefore a difference in material property. This is one reason why the 0.5" Ti-6Al-4V \*MAT\_224 model (Sean Haight, Leyu Wang, Paul Du Bois, Kelly Carney, Cing-Dao Kan, 2015) may not accurately predict the material property of 0.25" plate. The 0.25" Titanium plate has significantly more asymmetry than the 0.5" plate, or the other plates tested by this project (Hammer, 2012). Therefore the 0.25" Titanium plate was selected to be modeled with \*MAT\_224\_GYS. (GYS is an acronym for Generalized Yield Surface.)

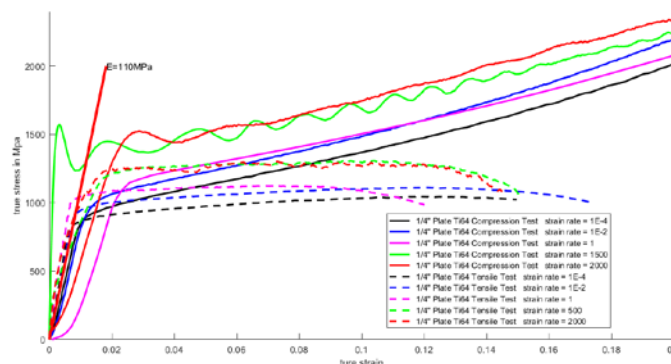


**Figure 1.** Experimental result of tension compression asymmetry for 1/4" Ti-6Al-4V plate under different strain rate. Force displacement relation is normalized to true strain and true stress with classical formula to contour the geometric difference. They do not represent the actual stress-strain relation.

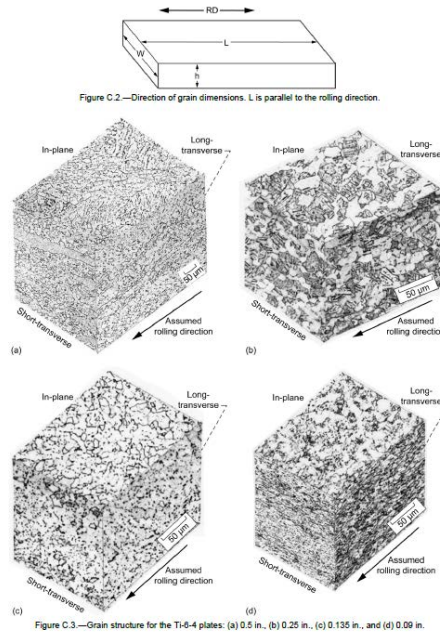


Figure 2. Grain Structure for the Ti-6Al-4V plate of (a) 0.5inch (b) 0.25 inch (c) 0.135 inch (d) 0.09 inch(Hammer, 2012)

\*MAT\_224\_GYS is an isotropic elasto-visco-plasticity model with a J3 dependent yield surface. Using J3 rather than J2 flow theory allows for tensile/compressive asymmetry in the material response. The elastic model is identical to the linear hyperelastic model(LIVERMORE SOFTWARE TECHNOLOGY CORPORATION (LSTC), 2016)

$$\mathbf{s} = 2G\dot{\boldsymbol{\epsilon}} \tag{1.1}$$

$$p = -K \ln V \tag{1.2}$$

where  $\mathbf{s}$  is the co rotational rate of the deviatoric Cauchy stress tensor.  $\dot{\boldsymbol{\epsilon}}$  is the Eulerian strain rate tensor.  $G$  and  $K$  are the elastic shear and bulk moduli, respectively. The plasticity model is a tabulated rate and temperature dependent material law (r.f. Equation 1.3).

$$\boldsymbol{\sigma} = f(\boldsymbol{\epsilon}_p, \dot{\boldsymbol{\epsilon}}_p, T) \tag{1.3}$$

where  $\boldsymbol{\sigma}$  is the Cauchy stress tensor,  $\boldsymbol{\epsilon}_p$  is the plastic strain tensor,  $\dot{\boldsymbol{\epsilon}}_p$  is the strain rate tensor,  $T$  is the temperature.

The terminology is identical to that of the\*MAT\_224 model except the input parameters can be defined separately for tension, compression and shear. The \*MAT\_224 input consists of two tables which define the rate and temperature dependent stress-strain behavior. Instead of two input tables, \*MAT\_224\_GYS allows for six input tables defining the rate and temperature dependency for tension, compression, and shear. The material model has an internal convexity check routine that will automatically modify the input curves if the yield surface, resulting from the tension, compression and shear yield stresses, is not convex. If the yield surface is not convex, non-unique solutions may result. The material model will automatically fill the table with no input by assuming the isotropic behavior on that particular direction.

The material model has two options for defining the plasticity: The stress versus effective plastic stain or the stress versus plastic strain. These two sets of curves are identical in tension but are different in compression and shear(LIVERMORE SOFTWARE TECHNOLOGY CORPORATION (LSTC), 2016). Currently \*MAT\_224\_GYS only works correctly in effective plastic strain mode (IFLAG=1) with initial multiplier SFIEPM=2. The IFLAG=0 mode is in development. Defining the material model with respect to plastic strain or effective plastic strain does not have any advantage either way.

## 2. Material Modeling Process

The available mechanical test data for the 0.25" titanium plate are summarized. Tension and compression test series are carried out using five strain rates and five temperatures. A shear test series was not performed on this plate, therefore the shear table is left blank in the \*MAT\_224\_GYS. Compression curve fitting and tension curve fitting are carried out in sequence. Table 1 summarizes all of the tests that are used in the material modeling. It is worthwhile to mention that the nominal strain rate is used only to categorized the test. It does not represent the real strain rate of the material test. The real strain rate of each test is not constant. Before necking, the strain rate of the test is not constant due to the limitation of testing machine. After necking, the specimen is not uniform and the strain rate in the necked area naturally has a much higher strain rate value. The strain rates defined in the tension and compression input tables are related to the curves which result from the try and error iterations of their creation. They do not reference the nominal strain rate at all.

### 2.1 Compression test simulation

Compression tests of different strain rates and temperatures are simulated with mpp-dyna-8.0.0-d. A solid cylindrical specimen placed on a stationary platform is compressed with another moving platform (r.f. Figure 3). A linear elastic material model with steel material properties is used for the platforms. The fixed and moving boundary condition constrains only the very top and bottom nodes of the moving and stationary platforms, respectively. The elastic platform allows some deformation which approximates the test condition. The contact surfaces for both the platforms and the specimen are wrapped with a layer of null shell elements to improve the contact performance.

\*CONTACT\_AUTOMATIC\_SINGLE\_SURFACE is used to defined the contact between the null shell elements. A static coefficient of 0.05, dynamic coefficient of 0.04 and exponential decay coefficient of 0.001 is used to model the friction between the specimen and platforms. These parameters are chosen such that the deformed "barrel" shape of the simulation is similar to that of the test (r.f. Figure 4). The specimen and the platform is modeled with reduced integrated solid element (elform=1) with hourglass control 6.

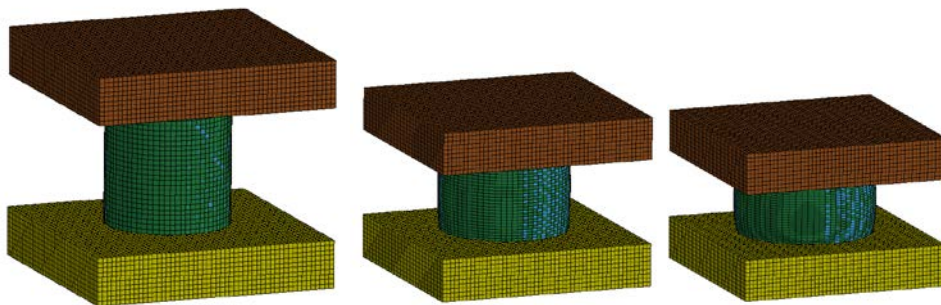


Figure 3 Compression Simulation Setup

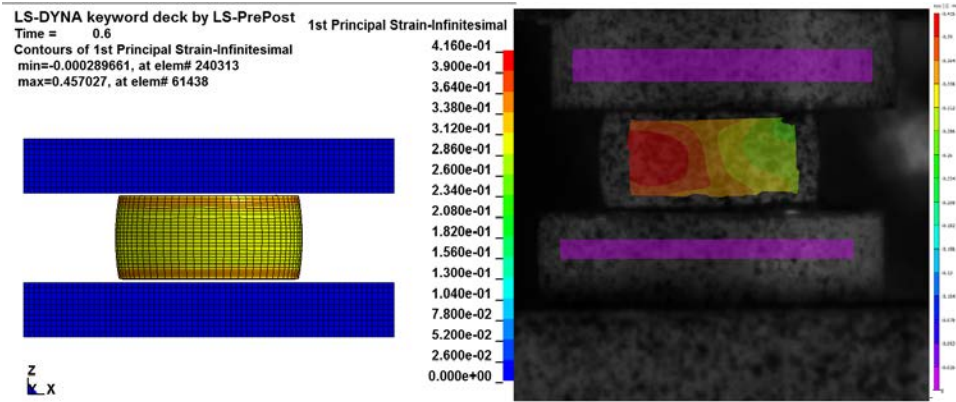


Figure 4 The first principle strain contour between test and simulation and the barrel shape comparison

## 2.2 Compression Test System Compliance Error Correction

In simulation, the cross-section force is measured at the center of the specimen. In physical test, the force data is measured from the testing machine. Since force is equilibrium, the force is directly comparable between test and simulation. In simulation, the displacement is measured at the very top and bottom node of the specimen. In test, the displacement is measured at the virtual DIC point on the platform instead of on the specimen (Hammer, 2012). This is due to the limitation of DIC. The cameras cannot capture the point on the edge. To make the displacement comparable to the simulation, the elastic deformation of the platform must be subtracted.

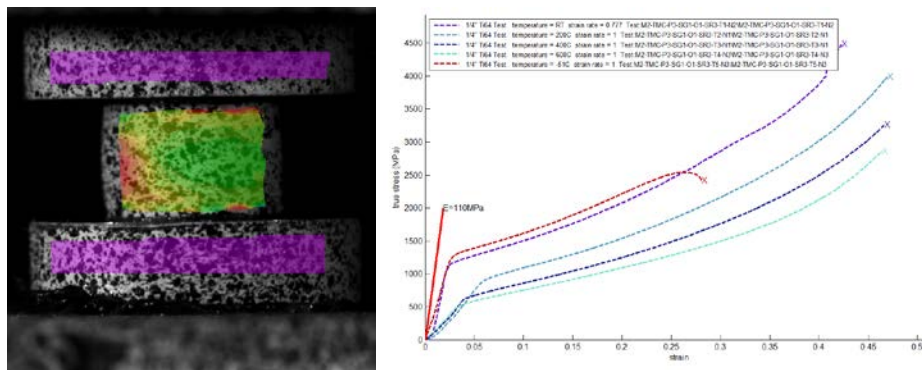


Figure 5 Left: DIC image shows the platform deformation. Right: strain stress relations show Young's modulus mismatch (stress/strain are calculated directly from force displacement data for an easy visual comparison, this does not represent the actual stress strain relation in material model)

Consider a system with an elastic deformed fixture. The system can be simplified as a specimen and a linear spring compressed together in series (r.f. Figure 6).

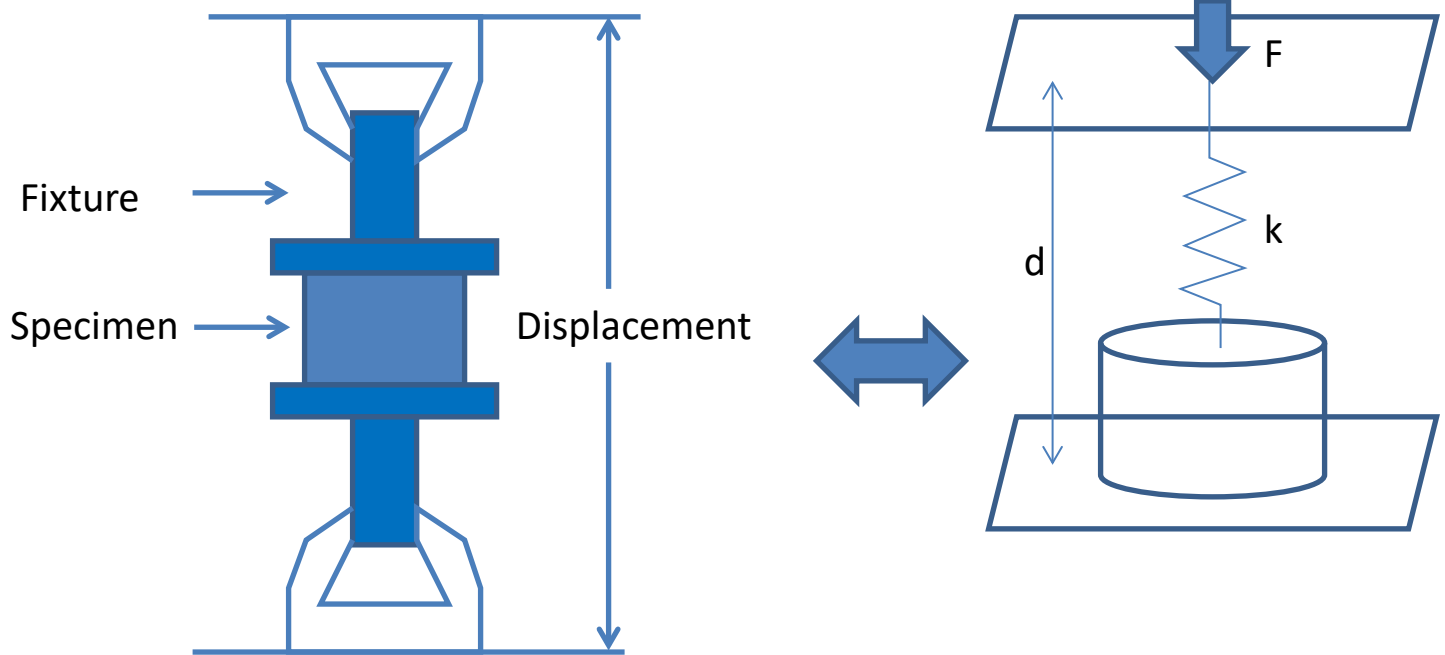


Figure 6 Fixture Compliance Error Correction Simplification

The displacement of coupon  $\Delta L^{specimen}$

$$\Delta L^{specimen} = \Delta L - \Delta L^{spring} \tag{1.4}$$

with

$$\Delta L^{spring} = F / k \tag{1.5}$$

where  $\Delta L^{spring}$  and  $\Delta L$  denotes the linear spring displacement and total displacement, respectively. To calculate the spring constant  $k$ , we take force at yield point  $f_y$  and displacement at yield point  $\Delta L_y$ . The yield strength

$$\sigma_y = \frac{f_y}{A} \tag{1.6}$$

where  $A$  is the original cross-sectional area. Notice that the Young's modulus  $E$  defines the relationship between true stress and true strain. A small iterative loop is used to determine the engineering yield strain.

set  $\epsilon_y = 0.1$

do  $\{s_y \leq \sigma_y (1 + \epsilon_y),$

$$e_y = s_y / E \tag{1.7}$$

$$\epsilon_y = \exp(e_y) - 1\}$$

until converge

where  $e_y$  and  $s_y$  are the yield true strain and yield true stress, respectively. The engineering yield strain and engineering yield true stress are  $\epsilon_y$  and  $\sigma_y$ , respectively. The displacement at the yield of the specimen is

$$\Delta L_y^{specimen} = \epsilon_y L_y^{specimen} \tag{1.8}$$

Therefore, the displacement of the fixture at the yield point is

$$\Delta L_y^{fixture} = \Delta L_y - \Delta L_y^{specimen} = \Delta L_y - \epsilon_y L_y^{specimen} \tag{1.9}$$

So, the spring constant can be calculated as

$$k = \frac{f_y}{\Delta L_y^{fixture}} = \frac{f_y}{\Delta L_y - \epsilon_y L_y^{specimen}} \tag{1.10}$$

The actual displacement of the specimen is

$$\Delta L_{coupon} = \Delta L_{total} - F / k \tag{1.11}$$

If a small strain assumption is adopted then,

$$\epsilon_y = \frac{\sigma_y}{E} \tag{1.12}$$

and an explicit formula of corrected displacement becomes available

$$\begin{aligned} \Delta L^{specimen} &= \Delta L^{total} - \frac{F}{k} = \Delta L^{total} - F \frac{\Delta L_y - \epsilon_y L_y^{specimen}}{f_y} \\ &= \Delta L^{total} - F \frac{\Delta L_y - L_y^{specimen} \sigma_y / E}{f_y} \\ &= \Delta L^{total} - F \frac{\Delta L_y - L_y^{specimen} F_y / AE}{f_y} \end{aligned} \tag{1.13}$$

Now the displacement history can be converted to the displacement of the specimen and is comparable to the simulation. For tests with little or no platform deformation, the correction method makes very little effect. (r.f. Figure 4). For test cases with visual deformation on the platform (r.f. Figure 5), the corrected displacement has a significant difference from the original displacement (r.f. Figure 7).

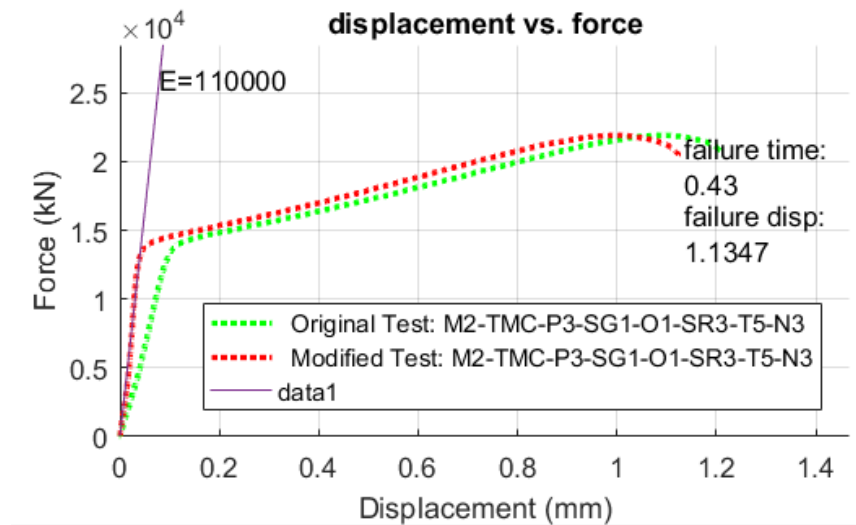


Figure 7 Sample Result of fixture compliance error correction

### 2.3 Temperature Scaled Method

The coupling of \*MAT\_224\_GYS with the LS-DYNA thermal solver is still in the development stage. This work only used the mechanical solver. By default, \*MAT\_224\_GYS compute temperatures even in the mechanical solver. Without the thermal solver, this represents an adiabatic heat condition; where the heat generated by plasticity has no time to dissipate.

A temperature scaling method is implemented to simulate temperature effects of the elevated temperature tests. The number of interpolation points on the \*CONTROL\_SOLUTION card (LCINT) needs to be set to a high value for the accurate rediscrization of the curves. The temperature setting on the \*MAT\_224\_GYS card (TR) is set to the desired temperature (r.f. Figure 8). The temperature table (LCKT and LCCT) is left unchanged. The new strain rate table for tension(LCK1) is scaled with a factor

$$\sigma_y^{lck1}(\varepsilon_p, \dot{\varepsilon}_p) = \sigma_y^{lck1}(\varepsilon_p, \dot{\varepsilon}_p) \frac{\sigma_y^{lckt}(\varepsilon_p, T_{current})}{\sigma_y^{lckt}(\varepsilon_p, T_{RT})} \quad (1.14)$$

where  $\sigma_y^{lck1}(\varepsilon_p, \dot{\varepsilon}_p)$  is the new strain rate table for tension. The function  $\sigma_y^{lckt}(\varepsilon_p, T_{current})$  is the curve of the desired temperature. The function  $\sigma_y^{lckt}(\varepsilon_p, T_{RT})$  is the curve for the room temperature. Similarly, the new strain rate table for compression (LCCR) is scaled with a factor

$$\sigma_y^{lccr}(\varepsilon_p, \dot{\varepsilon}_p) = \sigma_y^{lccr}(\varepsilon_p, \dot{\varepsilon}_p) \frac{\sigma_y^{lcct}(\varepsilon_p, T_{current})}{\sigma_y^{lcct}(\varepsilon_p, T_{RT})} \quad (1.15)$$

where  $\sigma_y^{lccr}(\varepsilon_p, \dot{\varepsilon}_p)$  is the new strain rate table for tension. The function  $\sigma_y^{lcct}(\varepsilon_p, T_{current})$  is the curve of the desired temperature. The function  $\sigma_y^{lcct}(\varepsilon_p, T_{RT})$  is the curve of the room temperature. Notice that both the tension and compression have to be scaled together for this method to work. For the isothermal case where constant temperature is desired, the specific heat (CP) can be set to a very large value so the temperature will not raise during the plastic deformation. This large specific heat method is applied to the lower rate tests of 1E-4 (1/s) and 1E-2 (1/s) in compression and 1E-4 (1/s) test in tension. Notice that a limitation of this method is that it cannot simulate the condition in between isothermal and adiabatic. This condition occurs when the test strain rates are neither very high or very low. For this reason, the analytical fitting result for test with a 1 (1/s) strain rate does not match the test perfectly.

```
*CONTROL_SOLUTION
$# soln nlq isan lcint
   0   0   0 1000000

*MAT_TABULATED_JOHNSON_COOK_GYS_TITLE
scaled MAT224_GYS Ti64
$ mid ro e pr cp tr beta numint
  3.443E-006 110 0.342 590 473.15 1 1
$ lck1 lckt lcf lcg lch lci
 1000 2000 0 0 0 0
$ lccr lcct lcsr lcst iflag sfiepm niter
 3000 4000 0 0 1 2 100
```

Figure 8 Input Deck for temperature scale

## 2.4 Time Condensed Method

It is computationally very costly to use the LS-DYNA explicit solver to model low strain rate tests with a long time duration. The implicit solver is ideal for the long duration, lower strain rate tests. However, the integration of \*MAT\_224\_GYS with the implicit solver is still in the developmental stage. So currently, the explicit solver has to be used to simulate tests with low strain rate. A time condensed method was implemented to achieve shorter simulation times.

As in the temperature scaled method, LCINT on the \*CONTROL\_SOLUTION card is set to a very large number. For a simulation that runs N time faster, the time value (first column) of strain rate curves (LCK1 and LCCR) is scaled up N times and the displacement boundary condition is scaled up N times (r.f. Figure 9). The value N is defined as the condense factor. The method is valid only if the simulation converges. The condense factor has to be small enough so the result is the same as from lower condense factors. For example, if a condense factor of 1000 produces the same result as condense factor of 500 and 2000, then 1000 times faster is slow enough to not cause dynamic effects. The selection of the condense factor is made on a case by case basis, and it depends on the level of uniformity in the test and the simulation.

```

*CONTROL_SOLUTION
$# soln  nlq  isnan  lcint
   0    0    0 1000000

*DEFINE_TABLE
$  tbid  sfa  offa
 1000 1000
$      value  curveid
 0.0000001000      1001
 0.0000100000      1002
 0.0010000000      1003

*DEFINE_CURVE
$  LCID  SIDR  SFA  SFO  OFFA
  97    0.001

$      A1      O1
 0.0000000000 -0.0000000000
36.1635774882 -0.0640549669

*DEFINE_TABLE
$  tbid  sfa  offa
 3000 1000
$      value  curveid
 0.0000001000      3001
 0.0000100000      3002
 0.0010000000      3003

```

Figure 9 Sample Input Deck for time condense factor 1000.

## 2.5 Tension Simulations Setup

The tension specimen has the shape of the dog-bone (r.f. Figure 10). For lower strain rate tests of 1E-4, 1E-2 and 1 (1/s), the test is performed on a Instron test frame. The moving grip at the top pulled the specimen upward while the bottom grip holds the specimen fixed. The force is measured by the test frame and the displacement were measured by DIC. Data was provided at a virtual strain gauge with a length of 4mm, which is marked with a white dot in Figure 10. Notice that the displacement was provided at the 4mm virtual strain gauge points, not at the end of the specimen where the grip is fixed. However, in the simulations the displacement boundary condition is specified at the end of the test section of the specimen (at the edge of the picture in Figure 10). This difference in boundary condition locations makes little difference for the lower strain rate cases.

For higher strain rates of 500 (1/s) and 1000 (1/s), the tests are performed on a split Hopkinson bar. Because the dynamics effects are large in a split Hopkinson bar test, a little change in boundary condition will cause large differences in the strains of the necking region. In split Hopkinson bar tests, the constrained end of the test specimen is not completely fixed. So, ideally the displacement history of two additional, further apart DIC points would be used for the boundary conditions. However, this data is not yet available for the 0.25" Titanium plate higher rate tension tests. For the higher strain rate tests, the second-best method was used to apply boundary conditions directly at the 4mm virtual DIC point and also compare the test and simulation at these points.

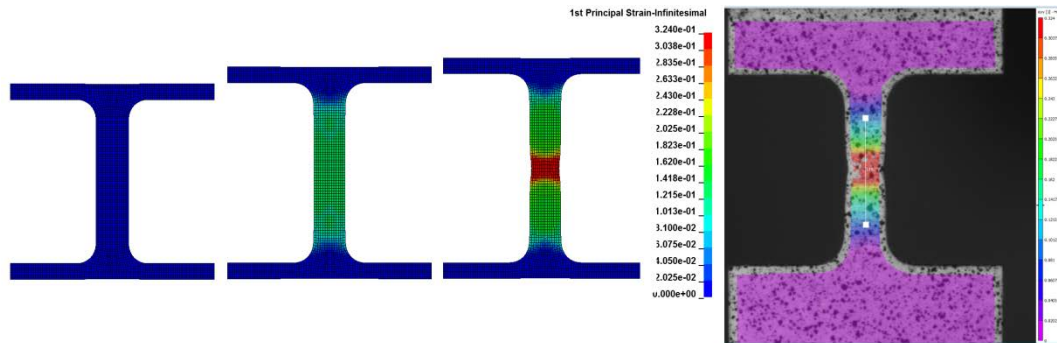


Figure 10 Simulation Setup (left) and the test photo with virtual DIC 4mm apart(right)

### 3. Preliminary Fitting result

The material model input is built with the iterative method described in the 0.5" Titanium report (Sean Haight, Leyu Wang, Paul Du Bois, Kelly Carney, Cing-Dao Kan, 2015). The analysis presented below and labeled "aa12\_attempt\_22" yields an overall good agreement with the test. Each test condition has three test repeats. This preliminary result picked one of the three available tests to compare for each condition. The final result will compare the force displacement, as well as the strain contour from DIC, for all three available tests and simulations.

Table 1 summarizes the special treatment applied to each test series, and these treatment are reviewed here. In Section 2.4, the Time Condensed Method was explained in detail. The time condense factor was chosen such that a converged simulation resulted. Compression has no necking therefore a larger time condense factor is allowed. In Section 2.3, the Temperature Scaled Method was explained in detail. This allowed the mechanical solver to simulate a test performed at elevated temperatures. For lower strain rate tests that are isothermal, an artificially large specific heat scaling factor is used to make the temperature almost constant. In tension, necking causes local heat generation and in the 1E-2 (1/s) strain rate test conduction is not fast enough for the test to be isothermal. For compression, the 1E-2 test is isothermal as the deformation is more uniform than in tension.

For the tension thermal tension series, notice that a mismatch is observed for -50C simulation at 1 (1/s) strain rate. It is possible that the test is neither isothermal nor adiabatic and so would require a coupled mechanical thermal solution to simulate. As presented in Section 2.5 Tension Simulations Setup, the tension high strain rate tests (500 (1/s) and 1000 (1/s)), the boundary conditions are directly placed on the DIC points. For compression, the displacement is measured at the platform. In Section 2.2 Compression Test System Compliance Error Correction, the method to subtract the system compliance error from test data was explained (r.f. Figure 15).

In Figure 11, the tables of the \*MAT\_224\_GYS input deck for 1/4" Ti-6Al-4V plate are plotted. Tests and simulations are compared for tension strain rate series, tension temperature series, compression strain rate series, and compression temperature series in Figure 12, Figure 13, Figure 14, and Figure 15, respectively.

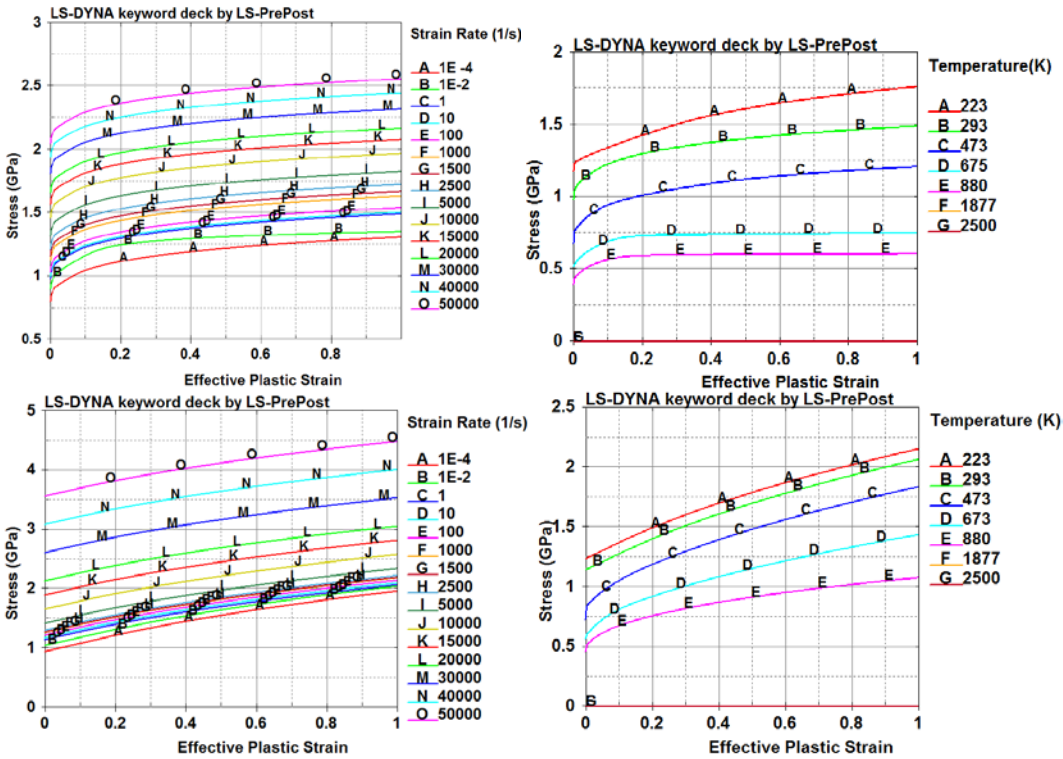


Figure 11. LS-DYNA \*MAT\_224\_GYS input Deck for 0.25" Ti-6Al-4V plate. tension strain rate table (Top Left). Tension temperature table (Top Right). Compression strain rate table (Bottom Left). Compression temperature table (Bottom Right). All tests are done at nominal strain rate = 1 (1/s).

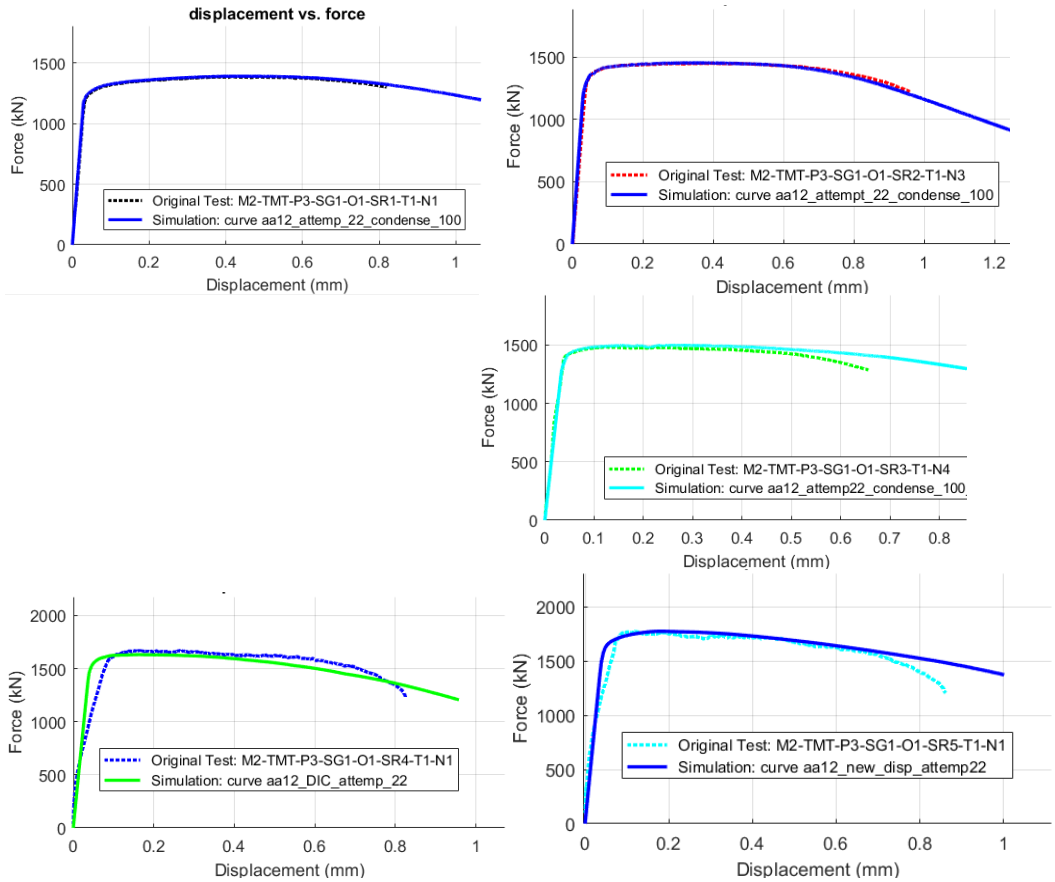


Figure 12 Simulation and test data comparison for Tension Strain Rate Series: 1E-4 (1/s) strain rate test (Top Left). 1E-2 (1/s) strain rate test (Top Right). 1 (1/s) strain rate test (Middle). 500 (1/s) strain rate test (Bottom Left). 1000 (1/s) strain rate test (Bottom Right). All strain rate is nominal, actual strain rate varies for each test. All test are at room temperature.

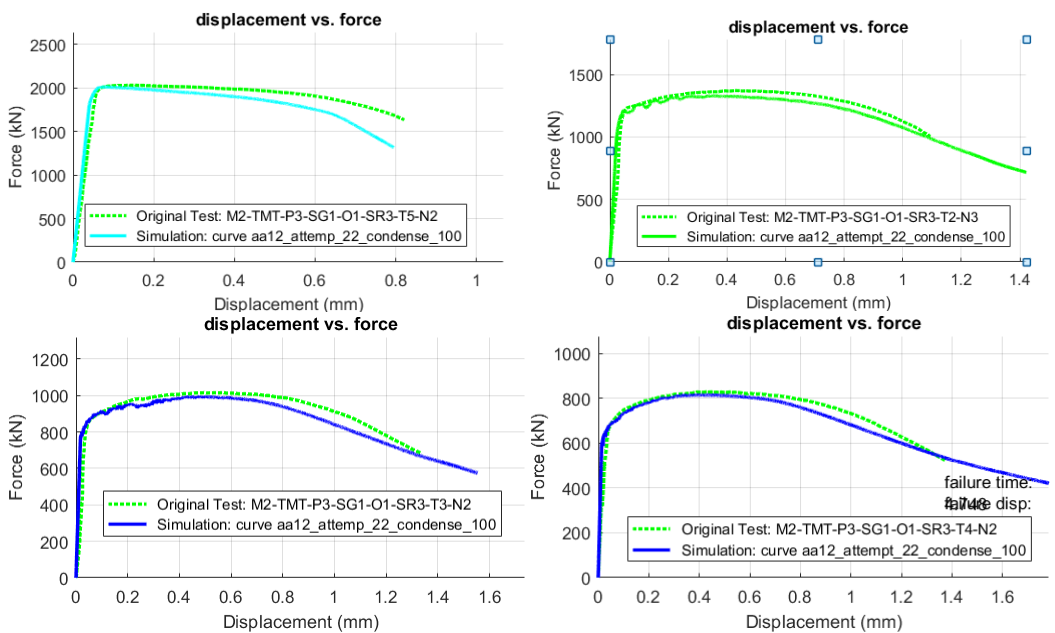


Figure 13 Simulation and test data comparison for Tension Temperature Series: -50C (Top Left). 200C (Top Right). (Middle Left). 400C (Bottom Left). 600C (Bottom Right). All tests are done at nominal strain rate = 1 (1/s).

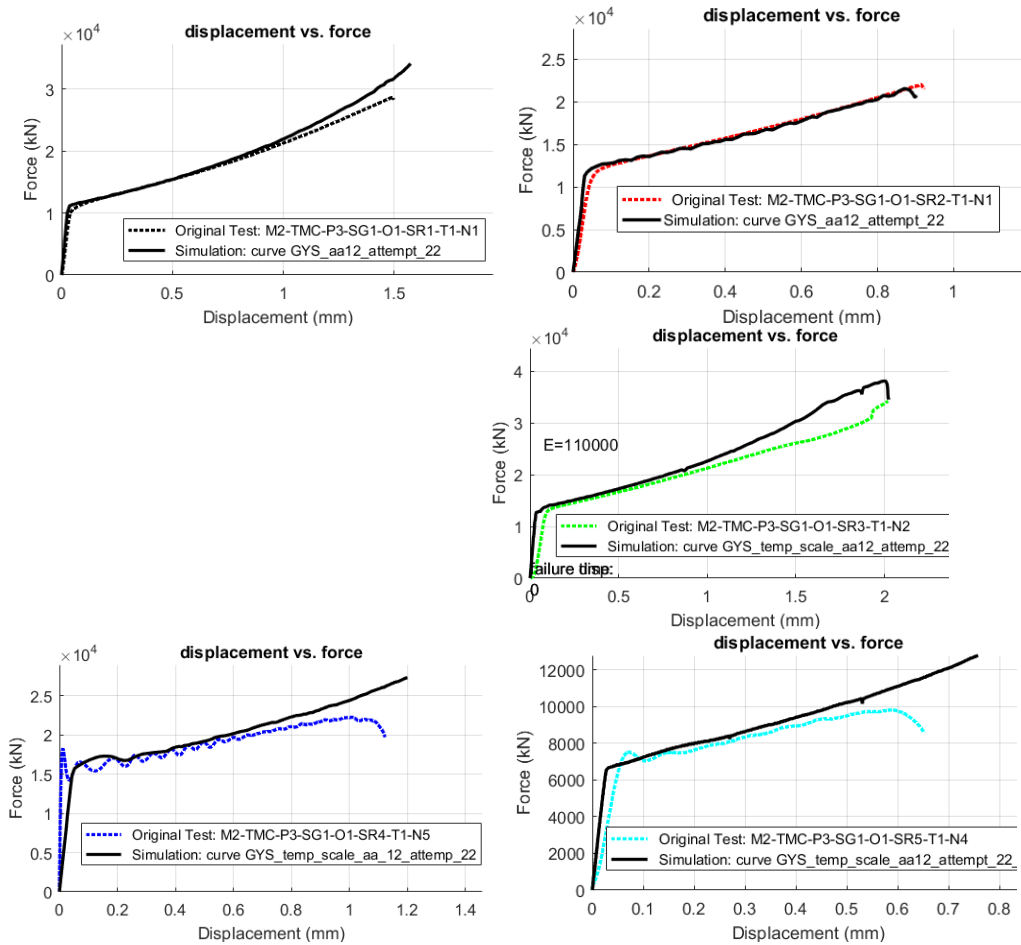


Figure 14 Simulation and test data comparison for compression strain rate series:  $1E-4$  (1/s) strain rate test (Top Left).  $1E-2$  (1/s) strain rate test (Top Right). 1 (1/s) strain rate test (Middle). 500 (1/s) strain rate test (Bottom Left). 1000 (1/s) strain rate test (Bottom Right). All strain rate is nominal, actual strain rate varies for each test. All test are at room temperature.

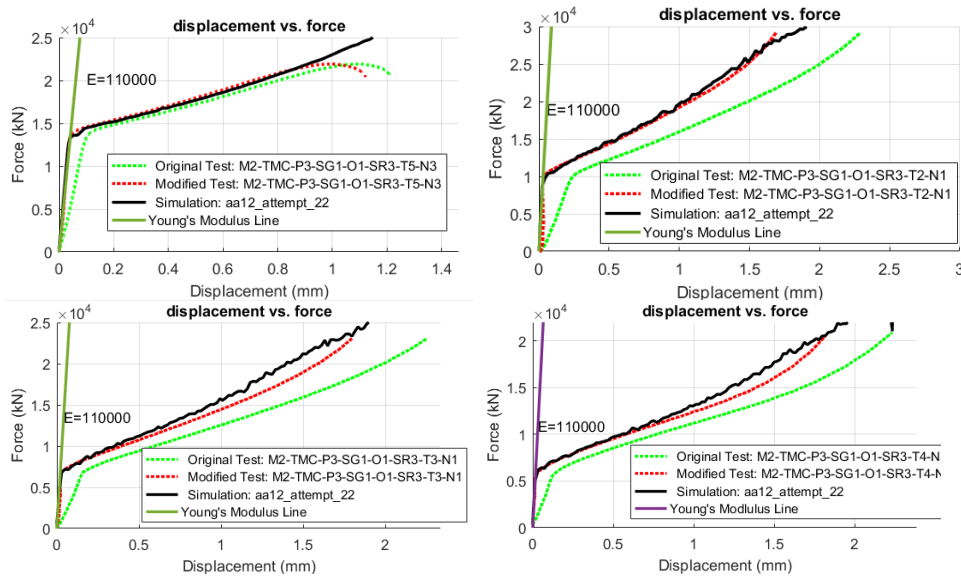


Figure 15 Simulation and test data comparison for Compression Temperature Series: -50C (Top Left). 200C (Top Right). 400C (Bottom Left). 600C (Bottom Right). All tests are done at nominal strain rate = 1 (1/s).

<i>Test (Direction/Strain Rate/Temperature)</i>	<i>Time Condense</i>	<i>Temperature Scale</i>	<i>Specific Heat Scale factor</i>	<i>Boundary Condition at the grip</i>	<i>Boundary Condition at the DIC Point</i>
<i>Tension 1E-4/RT</i>	<i>1E6</i>	<i>No</i>	<i>1E6</i>	<i>Yes</i>	<i>No</i>
<i>Tension 1E-2/RT</i>	<i>1E4</i>	<i>No</i>	<i>1</i>	<i>Yes</i>	<i>No</i>
<i>Tension 1/RT</i>	<i>1E2</i>	<i>No</i>	<i>1</i>	<i>Yes</i>	<i>No</i>
<i>Tension 500/RT</i>	<i>1</i>	<i>No</i>	<i>1</i>	<i>No</i>	<i>Yes</i>
<i>Tension 1000/RT</i>	<i>1</i>	<i>No</i>	<i>1</i>	<i>No</i>	<i>Yes</i>
<i>Tension 1/-50C</i>	<i>1E2</i>	<i>Yes</i>	<i>1</i>	<i>Yes</i>	<i>No</i>
<i>Tension 1/200C</i>	<i>1E2</i>	<i>Yes</i>	<i>1</i>	<i>Yes</i>	<i>No</i>
<i>Tension 1/400C</i>	<i>1E2</i>	<i>Yes</i>	<i>1</i>	<i>Yes</i>	<i>No</i>
<i>Tension 1/600C</i>	<i>1E2</i>	<i>Yes</i>	<i>1</i>	<i>Yes</i>	<i>No</i>
<i>Compression 1E-4/RT</i>	<i>1E7</i>	<i>No</i>	<i>1E3</i>	<i>Yes</i>	<i>No</i>
<i>Compression 1E-2/RT</i>	<i>1E5</i>	<i>No</i>	<i>1E3</i>	<i>Yes</i>	<i>No</i>
<i>Compression 1/RT</i>	<i>1E3</i>	<i>No</i>	<i>1</i>	<i>Yes</i>	<i>No</i>
<i>Compression 500/RT</i>	<i>1</i>	<i>No</i>	<i>1</i>	<i>Yes</i>	<i>No</i>
<i>Compression 1000/RT</i>	<i>1</i>	<i>No</i>	<i>1</i>	<i>Yes</i>	<i>No</i>
<i>Compression 1/-50C</i>	<i>1E3</i>	<i>Yes</i>	<i>1</i>	<i>Yes</i>	<i>No</i>
<i>Compression 1/200C</i>	<i>1E3</i>	<i>Yes</i>	<i>1</i>	<i>Yes</i>	<i>No</i>
<i>Compression 1/400C</i>	<i>1E3</i>	<i>Yes</i>	<i>1</i>	<i>Yes</i>	<i>No</i>
<i>Compression 1/600C</i>	<i>1E3</i>	<i>Yes</i>	<i>1</i>	<i>Yes</i>	<i>No</i>

*Table 1 Summary of the special treatment applied to each test series*

### 3. Conclusion

It is demonstrated that the \*MAT\_224\_GYS is suitable to model the tension compression asymmetry observed in 0.25" Ti-6Al-4V plate. Preliminary result shows that a single input deck is able to predict all the material tests of different strain rates and temperatures in both tension and compression.

### Acknowledgments

The authors would like to thank William Emmerling and Daniel Cordasco of the Federal Aviation Administration of the U.S. Department of Transportation for their support of this research.

### References

- Eringen, A.C., 1980. Mechanics of Continua, 2nd edition. ed. Krieger Pub Co, Huntington, N.Y.
- Hammer, J.T., 2012. Plastic deformation and ductile fracture of Ti-6Al-4V under various loading conditions. The Ohio State University.
- Liu, I.-S., 2002. Continuum Mechanics, Advanced Texts in Physics. Springer Berlin Heidelberg, Berlin, Heidelberg.
- LIVERMORE SOFTWARE TECHNOLOGY CORPORATION (LSTC), 2016. LS-DYNA KEYWORD USER'S MANUAL VOLUME II Material Models, r:7155.
- Sean Haight, Leyu Wang, Paul Du Bois, Kelly Carney, Cing-Dao Kan, 2015. Development of a Titanium Alloy Ti-6Al-4V Material Model Used in LS-DYNA.